Dispersed Oil–Water–Gas Flow Through a Horizontal Pipe

K. Piela, R. Delfos, G. Ooms, and J. Westerweel
J.M. Burgerscentrum for Fluid Mechanics, Delft University of Technology,
Laboratory for Aero- and Hydrodynamics, Leeghwaterstraat 21, 2628 CA Delft, The Netherlands

R.V.A. Oliemans
J.M. Burgerscentrum for Fluid Mechanics, Delft University of Technology, Kramers Laboratory,
Prins Bernhardlaan 6, 2628 BW Delft, The Netherlands

DOI 10.1002/aic.11742
Published online March 23, 2009 in Wiley InterScience (www.interscience.wiley.com).

An experimental study of three-phase dispersed flow in a horizontal pipe has been carried out. The pressure drop over the pipe strongly increases with increasing bubble and drop volume fraction. Because of the presence of drops the transition from dispersed bubble flow to elongated bubble flow occurs at a lower gas volume fraction. The gas bubbles have no significant influence on the phase inversion process. However, phase inversion has a strong effect on the gas bubbles. Just before inversion large bubbles are present and the flow pattern is elongated bubble flow. During the inversion process the bubbles break-up quickly and as the dispersed drop volume fraction after inversion is much lower than before inversion, a dispersed bubble flow is present after inversion. (When inversion is postponed to high dispersed phase fractions, the volume fraction of the dispersed phase can be as high as 0.9 before inversion and as low as 0.1 after inversion.) © 2009 American Institute of Chemical Engineers
AIChE J, 55: 1090–1102, 2009
Keywords: dispersed flow, oil–water–gas flow, phase inversion, horizontal pipe, bubble sizes

Introduction

In the oil industry oil–water–gas flow often occurs. For instance, when producing oil from a subsurface reservoir it is very well possible that not only oil but also water and gas (present in the reservoir) flow through the production tubing to the facilities at the surface. To predict the production rate it is essential to know the properties of such a three-phase flow and to be able to model it. There are not many papers dealing with three-phase flow through a pipe, but recently this subject is receiving more attention because of the industrial relevance. The flow pattern as function of the flow conditions was studied.[1–4] Also the influence of the inclination angle of the pipe on the flow was investigated.[5] It has been shown that the pressure drop of the three phase oil–water–gas system is of the same order of magnitude as the pressure drop of a two-phase system consisting of the gas and the dominating liquid phase.[6] Lahey et al.[7] applied the drift-flux technique and validated it against volume fractions data for such a flow. Furthermore, Hewitt[8] showed the importance of the mixing process on the flow behavior.

In our research, we have restricted ourselves to dispersed three-phase flow with a continuous liquid (oil or water), in which drops of the other liquid and gas bubbles are present. Dispersed flow occurs only at high mixture velocities. Special attention was given to the phenomenon of phase inversion, whereby the mixture switches from an oil-continuous phase (with water drops and gas bubbles) to a water-continuous

Correspondence concerning this article should be addressed to G. Ooms at g.ooms@tudelft.nl.

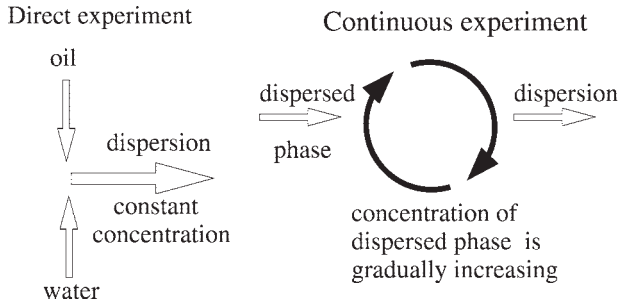

Figure 1. Sketch of the direct and continuous experiments.

phase (with oil drops and gas bubbles), or vice versa. During phase inversion the pressure gradient of the three-phase flow in the pipe increases strongly. So it is important to know at what conditions phase inversion occurs, in order to find out whether in practice it can be avoided or its effect on the pressure drop can be minimized.

In our previous studies,[9,10] we carried out experiments to study phase inversion in an oil–water flow through a pipe. Two different types of experiments were carried out (see Figure 1). During a direct experiment water and oil were pumped from separate tanks and injected simultaneously into the pipe at constant volume fractions. During a continuous experiment the dispersion was circulated through the pipe loop and the dispersed phase was gradually injected (while the same amount of dispersion was removed). So during a continuous experiment the dispersed phase fraction was slowly increasing up to the inversion point. The continuous experiments showed that phase inversion can be postponed to a high dispersed phase fraction (even as high as 0.9). Phase inversion was also found to be strongly dependent on the injected phase volume fraction (ratio of the volume flow rate of injected liquid and the volume flow rate of the mixture). One of the purposes of this further study was to investigate the influence of the presence of gas bubbles on the earlier results.

In section *Experiments* the experimental set-ups are described. Also the visualization technique using a high speed camera and an optical fiber probe will be discussed. In section *Oil–water dispersed flow* our previous results from the oil–water experiments are briefly summarized. Section *Gas–liquid dispersed flow* is devoted to gas–liquid dispersed flow. In section *Oil–water–gas dispersed flow* the results from the three-phase flow experiments are given with special attention to the influence of gas bubbles on the phase inversion process. Finally section *Conclusions* presents the most important conclusions.

Experiments

General information

An acrylic pipe with an inner pipe diameter of 16 mm was used. The two immiscible liquids used were tap water and Shell Macron EDM 110 oil (density 794 kg/m^3, kinematic viscosity at 20° 3.9 mm^2/s and oil–water interfacial tension 0.045 N/m). As gas phase nitrogen was used (nitrogen–water surface tension 0.072 N/m, nitrogen–oil surface tension 0.024 N/m). All experiments were performed at high Reynolds and Froude numbers to make sure, that always a fully dispersed flow was present (according to Brauner[11] a mixture velocity of 1.42 m/s is sufficient for our experimental conditions). Continuous and direct experiments were carried out; they will be explained in more detail later on. In both types of experiments the mixture velocity in the pipe was kept constant. Continuous experiments with water as the continuous phase were conducted at a mixture velocity of 3 m/s, which yields a Weber number of 3200. Continuous experiments with oil as the continuous phase were performed at a mixture velocity 3.5 m/s, which gives a Weber number of 3500. The Weber number, being far beyond unity, indicates that interfacial tension is far too weak to withstand inertia forces. Hence the liquid phases break up into a 'dispersed flow', in which one phase gets dispersed into the other continuous phase. The maximum stable bubble size as calculated by the relation of Hinze[12] is 0.13 mm and 0.12 mm, respectively. The details of the pipe configurations used for the two types of experiments will be given when these experiments are discussed.

Pressure drops were measured at different locations over a distance of 1 m. Differential pressure transducers (Validyne DP-15, measuring error <3%) were used and the pressure signal was sampled at a rate of 2 kHz. Data were averaged over 2000 samples. Conductivity measurements (at the same frequency) were done with a cell consisting of two (0.2 mm diameter) wire electrodes mounted in the pipe: one in the vertical direction and one in the horizontal direction. The distance between the electrodes in the center of the pipe was 2 mm. During the experiment we also monitored the temperature with a thermocouple mounted in the pipe wall. Most of the experiments were conducted more than at least two times and the reproducibility of the experiments was good.

Visualization with high-speed camera

To make a detailed study of the dispersion morphology, samples were taken from the flow by means of a 7 mm inner diameter sampling tube centered in the 16 mm inner diameter pipe loop. The sample tube liquid is led through a visualization cell (which consists of 2 glass plates 1 mm apart, leaving a channel of width 20 mm). The visualization cell was illuminated from the backside using a 500W halogen lamp, while a high-speed camera was used to take images at the front side. The camera was operated at a frame rate of 50 or 500 fps. A sketch of the sampling technique is given in Figure 2; more details are given in our previous paper.[9]

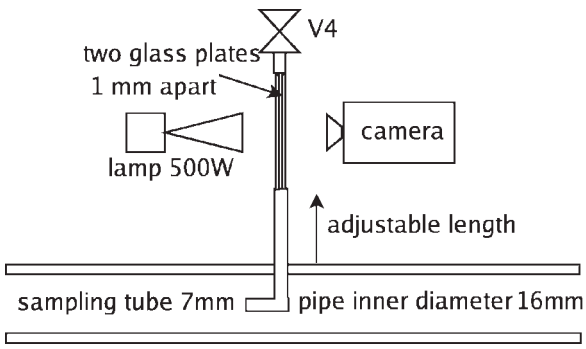

Figure 2. Sketch of the visualization method.

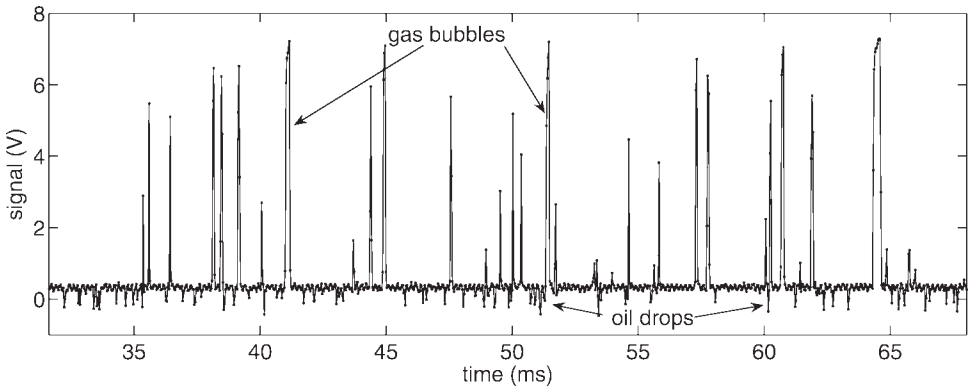

Figure 3. Signal from the optical probe for an oil–water–gas flow.

Water is the continuous phase (gas fraction is 0.07, oil volume fraction is 0.12 and mixture velocity 3 m/s). The presence of gas bubbles and oil drops can be observed.

To check whether this observation procedure had some influence on the dispersion morphology we performed experiments with various tube lengths between visualization cell and pipe, and at various sample liquid flow rates. We found little if any influence. We also changed the distance between the glass plates in the visualization cell from 1 mm to 5 mm; again the results were qualitatively the same, except that for the wider gap the observed mixture turns more opaque at higher dispersed phase volume fractions.

Optical fiber probe

At high mixture velocities the drops and bubbles were very small and the pipe flow became optically dense (opaque). Visualization by means of a (high-speed) camera was then not possible any more. To gather more information about the gas bubble size distribution a single-tip optical fiber probe was used.

The fiber probe consists of a glass rod (of 200 micron diameter), with a rounded tip (of tip radius 60 micron) inserted in the flow.[13,14] The probe is mounted radially traversable along the vertical (z) axis. The percentage of light led into the fiber reflected back from the tip is detected, and is a measure for the difference in refractive index between glass and the medium wetting the fiber tip. After appropriate thresholding or signal recognition, the actual phase wetting the probe, and related parameters such as bubble frequency or local void fraction can be derived. Probes of this kind for gas–liquid, liquid–liquid, and three-phase flows have been in use since the nineties.[15–19] In general, they lack the ability to detect phase elements that are small or bounce off. Furthermore, in liquid–liquid flows they tend to suffer most from the wetting phase sticking to the interface, as described by Fordham et al.[18,19] and Descamps et al.[20]

A typical probe signal for an oil–water–gas flow is presented in Figure 3. The refractive index of the gas is much lower than that of the two liquid, hence the gas bubbles can easily be discriminated from the probe signal. The difference in refractive index between the two liquids is much smaller, and only the bigger oil drops (lowest signal) can be separated from the measurement noise, which makes determination of the liquid distribution more questionable. For this reason we used the optical probe only to detect gas bubbles.

We used the fiber probe near the pipe centerline up to halfway the outer radius. The probe signal was sampled at a rate of 30 kHz; at a mixture velocity of 3 m/s and the presumably rather flat velocity profile, this gives an axial resolution of 0.1 mm. This is sufficiently small, while smaller bubbles will not be detected sufficiently anyway. With the given limitations of the optical probe system, we used the results in a qualitative way only, i.e. to compare bubble sizes between similar experiments (in which only one parameter was changed) and to observe the transition from the dispersed bubble flow pattern to the elongated bubble flow pattern (for which the average bubble size changes significantly). In this way the results of the optical fiber probe contributed well to the interpretation of the measurements.

Continuous experiments

A sketch of the set-up used for the continuous experiments is shown in Figure 4. The symbols used in the sketches have the following meaning: V, valves; F1, Krohne Optimass 7000 flow meter (measuring error $<0.26\%$); F2, Krohne Corimass E flow meter (measuring error $<0.4\%$); C1, conductivity cell; and T1, thermocouple. During the continuous experiments one of the liquids (water or oil) was taken from the continuous phase tank (see Figure 4) by means of Pump 1 and recirculated through the pipe. Pump 1 is a positive displacement pump (lobe pump), chosen to minimize the pumping effect on the dispersion morphology. After recirculating the liquid for a few minutes to ensure that the pipe walls were wetted by the liquid, injection of the other liquid started by pumping (using Pump 2) the dispersed phase through the injector into the pipe loop. During the injection Valve 2 was open and the same volume of dispersion liquid was removed from the pipe loop as the volume that was injected. When the desired dispersed-phase volume fraction was reached the injection by means of Pump 2 was stopped and injection of gas was started. Nitrogen gas was used, which was stored in a gas bottle (pressurized at 180 bar with a reduction to 6 bar). The gas flow was monitored by a rotameter. Flow meter 1 measured the density and the flow rate of the mixture in the pipe loop. The mixture velocity was kept constant during the experiment by an electronic feedback system (Pump 1 was controlled based on

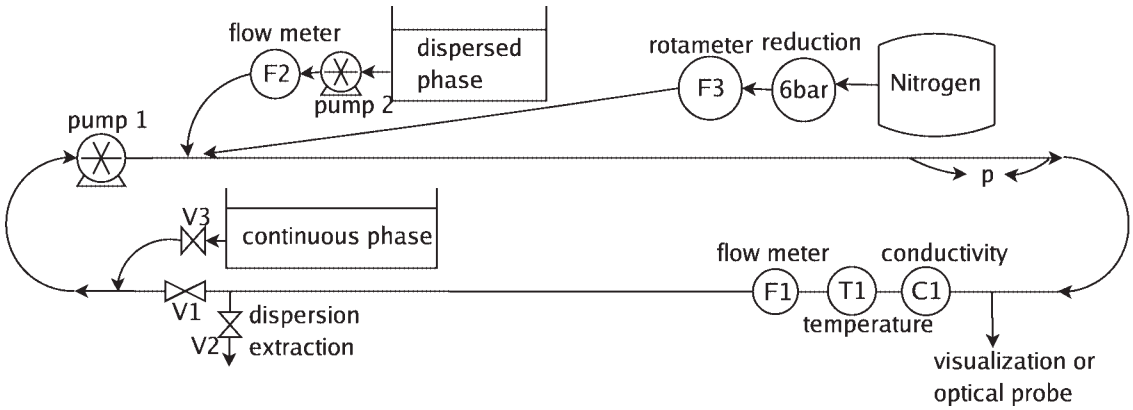

Figure 4. Sketch of the experimental set-up for continuous experiments.

measurements of flow meter 1). To study the influence of the length of the pipe loop also continuous experiments were carried out, whereby the pipe loop was significantly reduced in length. During these experiments the mixture circulates more often through the pump. However, we observed no difference in the results when compared with the results of the experiments carried out in the longer pipe loop.

A cylindrical container (placed around the pipe loop) with a number of holes in it was used as injector. The dispersed phase was pumped through the holes into the pipe loop. Three different types of injectors were used, viz. a container with 2 holes of 2 mm diameter, a container with 8 holes of 2 mm diameter, and one with 100 holes of 3 mm diameter (for more details, see Ref. 9). The experimental results were independent of the injector type. The pressure drop over one meter of pipe, p, was measured 5 m (313d) downstream of the injector.

Direct experiments

During the direct experiments water, oil and gas were taken from the three tanks and injected simultaneously by means of Pump 1, Pump 3 and rotameter into the pipe (see Figure 5). The mixture was injected at a constant phase fractions for at least 40 s. Flow meter 1 measured the density and the flow rate of the mixture in the pipe. The pressure drops p1..p6, again over 1 meter of pipe, were measured at six different positions: immediately downstream of the inlet and at distances of 2.0 m (125d), 5.0 m (315d), 11.7 m (730d), 18.7 m (1170d), and 26.5 m (1655d) from the inlet (where d is the pipe diameter).

Oil–water dispersed flow

In our previous experimental studies,[9,10] many phase inversion experiments were performed in an oil–water flow through a pipe. In this section we briefly summarize the results. We think that this will help in the interpretation of the experiments with gas injection, which will be presented in the coming sections.

In our earlier work results from continuous experiments and direct experiments were compared. As mentioned in the preceding paragraph during continuous experiments the dispersed phase was gradually added to the flowing mixture in the closed pipe loop. The dispersed phase fraction was slowly increasing and at a certain moment inversion occurred. During these experiments it was noticed that the dispersed phase fraction at which inversion occurs, depends

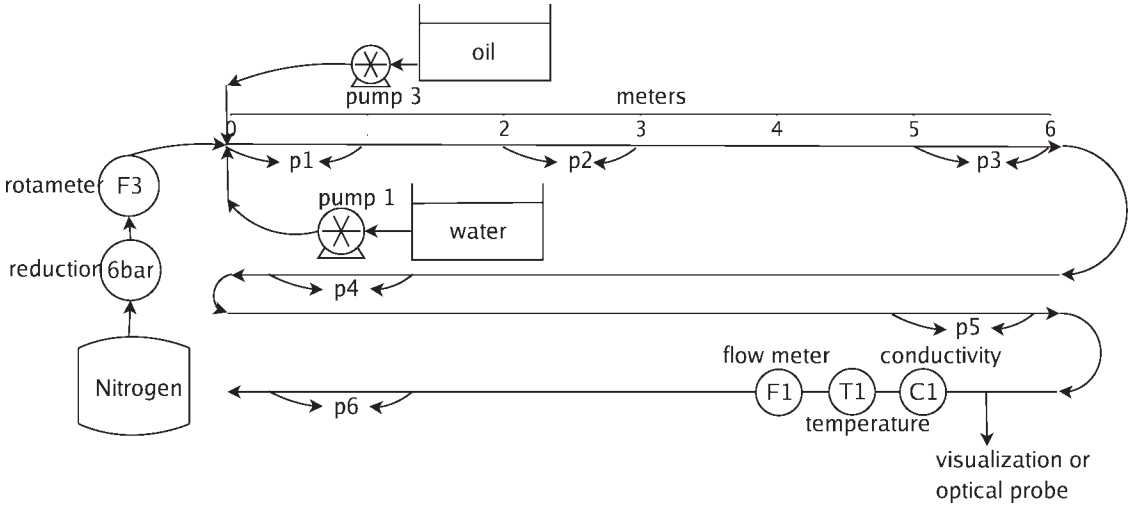

Figure 5. Sketch of the experimental set-up for direct experiments.

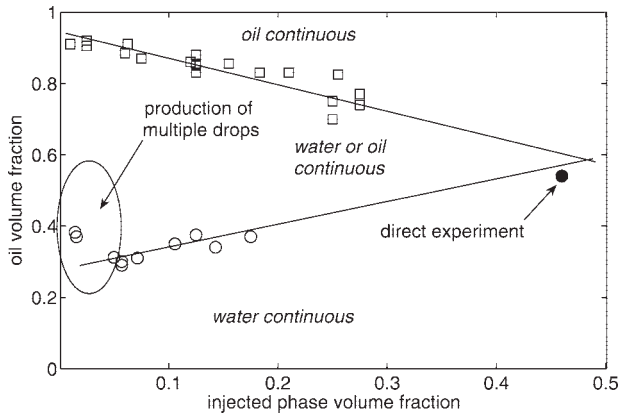

Figure 6. Inversion map.

The upper line gives the oil volume fraction at the point of inversion as measured during water-to-oil continuous experiments. The lower lines represent the oil volume fraction at inversion as measured during oil-to-water continuous experiments. The region in between the two lines is the ambivalence region, where both oil and water can be the continuous phase. Also the oil volume fraction at inversion as measured during the direct experiments is indicated.

almost linearly on the injected phase volume fraction χ (ratio of the volume flow rate of the injected liquid and the volume flow rate of the mixture).

For continuous experiments a so-called ambivalence region exists, in which both phases may be found to be continuous. Only outside this region one phase is always continuous and the other is always dispersed. Within the ambivalence region either one of the two phases can be continuous and the exact value at which phases invert depends on the operating conditions. By starting an experiment with pure water and gradually adding oil and by starting with pure oil and gradually adding water the ambivalence region was measured. It was found that the ambivalence region is almost independent of the Reynolds-, Froude-, and Weber number and also independent of the injection velocity of the dispersed phase [as long as the mixture velocity is sufficiently large ($\geq$2 m/s)]. The measured ambivalence region is shown in Figure 6. As can be seen the width of the region depends much on the injected phase volume fraction χ. The measured results lie on two lines, one for the water-to-oil experiments and one for the oil-to-water experiments. (Two measurement points for the oil-to-water experiments do not coincide with the line. The explanation for this deviation is given in Piela et al.[9]; entrapment of the continuous phase (oil) into the dispersed phase (water) increases the effective dispersed phase fraction. If the volume fraction of oil present as oil droplets inside the water drops would be subtracted from the total oil volume fraction, the measurement points would likely fit the line.)

During the direct experiments the two liquids were injected (from separate tanks) simultaneously into the pipe. The phase inversion process was determined by the mixing between oil and water at and after the inlet. At the critical phase volume fraction water-continuous and oil-continuous regions were created simultaneously. These regions interact flowing downstream. The interaction was very similar to the one observed during the inversion process during the continuous experiments. The direct experiment can be considered as a limiting case of the continuous experiment, with a large injection phase volume fraction of the dispersed phase and with inversion taking place before one cycle through the pipe loop is completed. No ambivalence region was observed during the direct experiments.

In Figure 7 the measured results for the friction factor $f = \frac{2\Delta P d}{\rho u^2 L}$ (ΔP is the pressure drop over a distance L) for water-to-oil and oil-to-water continuous experiments and for direct experiments are presented as a function of the dispersed phase volume fraction. As can be seen for continuous experiments the friction factor increases with increasing dispersed phase volume fraction, until it reaches its maximum during phase inversion after which it decreases significantly. During direct experiments an increase in pressure drop was observed at a dispersed phase volume fraction between 0.5 and 0.6. At that oil volume fraction water-continuous and oil-continuous regions are simultaneously created during mixing process. Those regions flow downstream while interacting, which causes an increase of the friction factor. Similar experiments in a horizontal pipe were carried out by Ioannou et al.[21] They observed, that at the point of phase inversion the pressure drop as well as the conductivity were very unstable. Pal[22] observed a strong increase in effective viscosity at phase inversion during direct experiments in a pipe.

Gas–liquid dispersed flow

We started the gas experiments with the injection of nitrogen in a single liquid (water). At the high liquid velocities that we applied, dispersed bubble flow occurred at low enough values of the gas volume fraction. At volume fractions in the range of 0.25 to 0.30 a transition to elongated bubble flow or slug flow was observed, in agreement with literature results.[23,24] Figure 8 shows the gas fraction and bubble size as function of the vertical distance to the pipe center at three different locations for a water–nitrogen flow with a mixture velocity of 3 m/s. As can be seen from this figure even at a mixture velocity much higher than as used for the oil–water experiments, it is difficult to uniformly disperse the gas in the pipe due to the buoyancy force on the bubbles. At a low gas fraction small bubbles are evenly

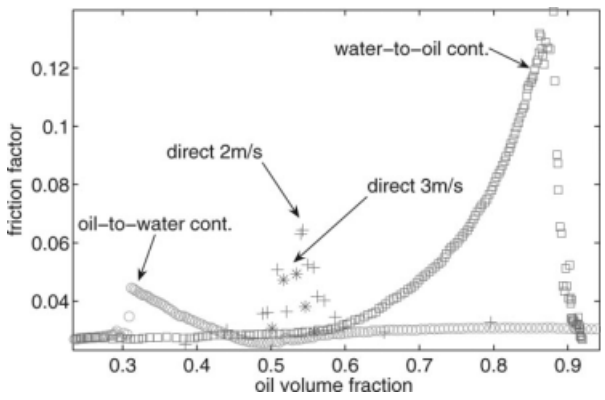

Figure 7. Friction factor as a function of oil volume fraction for continuous and direct experiments.

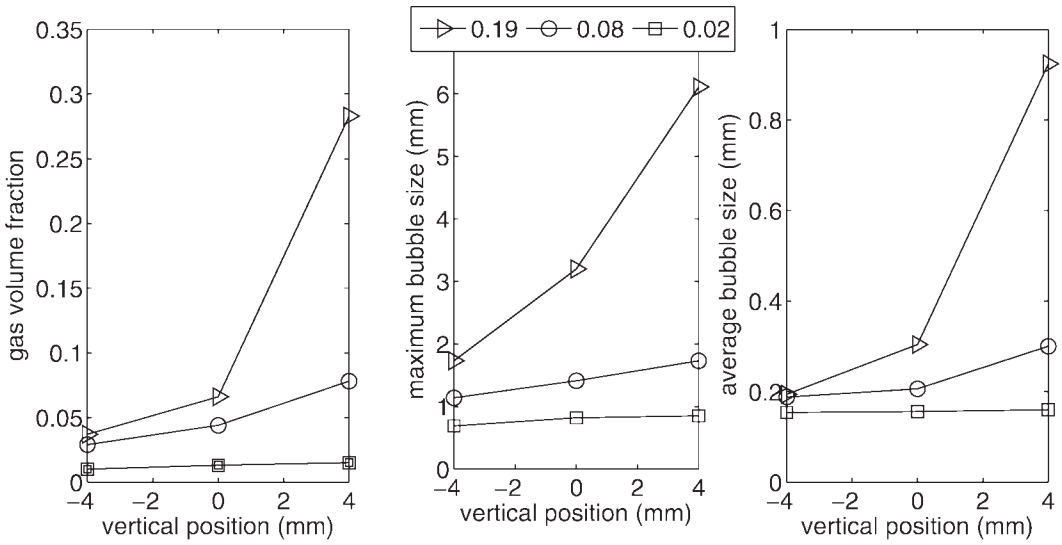

Figure 8. Gas volume fraction and bubble size in a cross section of the pipe at different average gas volume fractions for a mixture velocity of 3 m/s.

"0" indicates the pipe center, "−4" indicates 4 mm below the center, and "+4" is 4 mm above the center.

distributed in the pipe cross-section. However, at higher gas fractions large bubbles are created which tend to accumulate at the top of the pipe (leading to a transition to elongated bubble flow or slug flow).

Oil–water–gas dispersed flow

As mentioned in the introduction there is a limited number of studies dealing with three-phase flows. Some studies deal with the establishment of the flow pattern map. In our research, we concentrated our effort on the oil–water–nitrogen dispersed flow pattern. The continuous experiments were an extension of our previous oil–water experiments. The direct experiments were similar to the experiments performed by Descamps et al.[20,25] in a vertical pipe. Only in the horizontal pipe configuration (that we used) a higher mixture velocity had to be used to ensure dispersed flow.

Before starting the continuous and direct three-phase flow experiments we tried to find out, in which liquid phase the gas bubbles were present. To that purpose we performed a series of direct experiments, in which a liquid (oil or water) with nitrogen bubbles was injected simultaneously with the other liquid into the pipe. Therefore nitrogen was first dispersed into one of the liquids using an injection needle to ensure the generation of small bubbles. Thereafter this liquid–gas mixture was pumped together with the other liquid into the pipe. Figure 9 shows some pictures taken during these experiments. The top-left and bottom-left pictures show the results for an experiment, for which after the mixing process at the entrance to the pipe water has become the continuous phase with oil drops and nitrogen bubbles. In the top-right and bottom-right pictures oil is the final continuous phase with water drops and nitrogen bubbles. In the top pictures the volume fraction of the dispersed liquid phase is 0.07 and in the bottom pictures 0.15. The gas volume fraction is 0.03 for all cases. Because the refractive index between oil and water is small, the oil or water drops have a gray interface. However, the refractive index between oil and gas or between water and gas is much larger, which causes a black gas-liquid interface. This property allows us to easily recognize bubbles and drops in the pictures. We found that in the pipe the gas bubbles are always in the continuous liquid phase after the mixing region in the entrance part of the pipe. Also for the case that the liquid with gas bubbles that is pumped into the pipe, becomes the dispersed liquid phase in the pipe. This is an important result. With increasing volume fraction of the dispersed liquid phase the gas bubbles tend to grow in size.

Continuous experiments

A continuous experiment was started by flowing the first liquid at a certain velocity through the pipe loop and then gradually increasing the volume fraction of the second liquid by injecting it (in the form of drops) at a certain flow rate into the first liquid. At a certain moment in time injection of the second liquid was stopped (when the desired dispersed phase volume fraction was reached) and injection of gas was started. The gas volume fraction was increased up to the moment that a transition to elongated bubble flow took place.

Continuous experiments with water as continuous phase

In the first series of continuous experiments water was the continuous phase with oil injected in it up to a certain volume fraction. As mentioned nitrogen gas was then injected into it up to the point of elongated-bubble flow formation. Figure 10 shows the measured friction factor for these experiments as function of the gas volume fraction for five different values (0.0, 0.1, 0.2, 0.36, and 0.55) of the oil volume fraction.

As can be seen the friction factor for the water–gas case (oil volume fraction is 0.0) is steadily increasing with gas

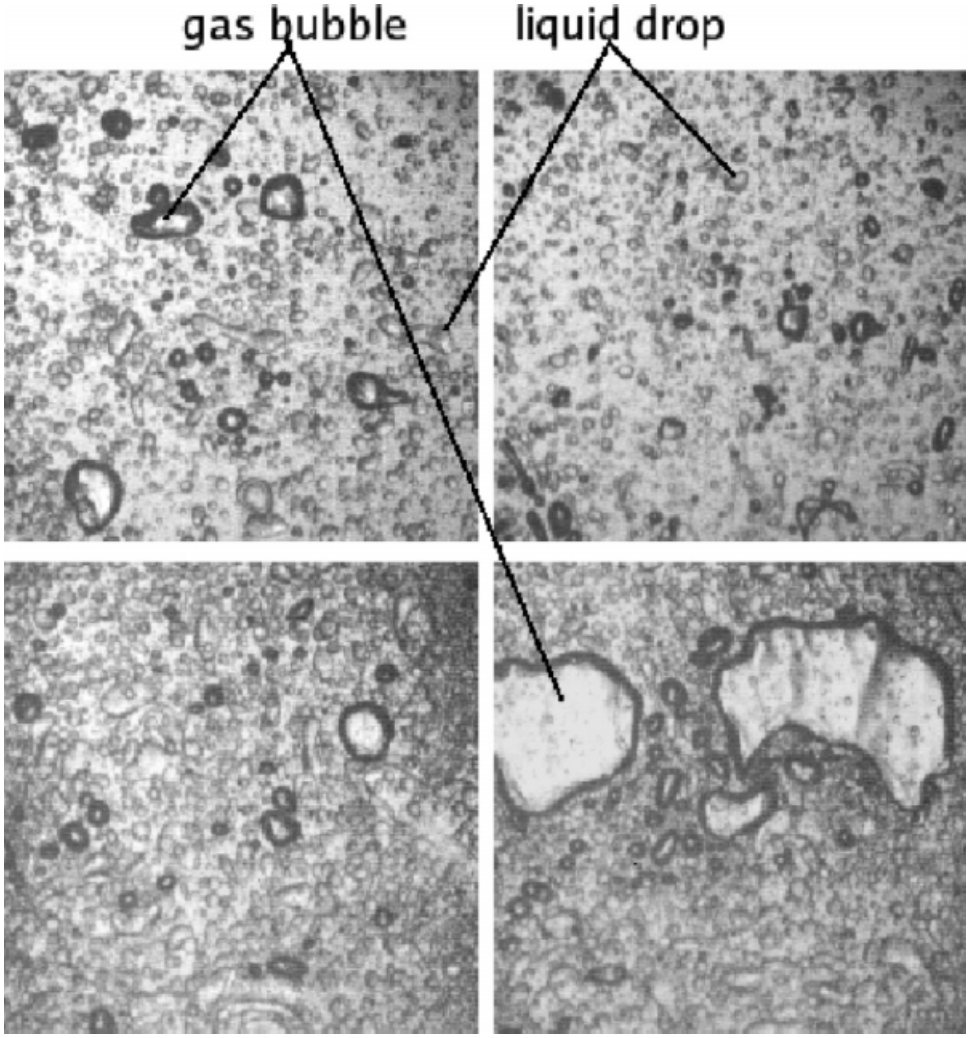

Figure 9. Gas bubbles are always found in the continuous liquid phase during a three-phase flow through a pipe.

In the left pictures water is the continuous phase; in the right pictures oil is the continuous phase.

volume fraction up to gas volume fraction of 0.3, at which point a very strong increase of the friction factor occurs. The maximum and average bubble size as measured by means of the optical fiber probe during the water–gas experiments are shown in Figure 11. The maximum bubble size is steadily increasing up to a gas volume fraction of 0.27, when large bubbles are created and the flow pattern is changing from dispersed bubble flow to elongated bubble flow. This is in the agreement with other experiments.[23]

Figures 10 and 11 show also the friction factor, maximum and average bubble size for water–oil–gas experiments at different oil volume fraction. Even a small volume fraction of oil (0.1) has already a significant influence on the transition of dispersed bubble flow to elongated bubble flow. This transition occurs at a lower gas fraction (around 0.16). This is perhaps surprising, as the friction factor for this case is larger than for the water–gas experiments and, therefore, break-up of bubbles could be expected to be easier than for the water–gas case. Obviously the oil drops avoid this from happening and stimulate the creation of large bubbles. Increasing the oil volume fraction to 0.2 and 0.36 does not change these results very much. The transition to elongated bubble flow was always measured to be close to a gas volume fraction of 0.16 and we found a further small increase in friction factor and bubble size. Only at much higher oil volume fraction of 0.55 there was a significant decrease again in the gas fraction where transition to elongated bubble flow took place. It is then almost impossible to create a dispersed bubble flow. Even the injection of a small amount of gas causes transition to elongated bubble flow. However, the injection of gas does not influence the oil drops. The oil drops are still dispersed in the water continuous phase.

Figure 12 shows similar results, only this time the mixture velocity has values of 2 m/s, 3 m/s, and 4 m/s and the oil volume fraction is 0.36. For a mixture velocity of 2 m/s the transition of dispersed bubble flow to elongated bubble flow occurs at a low gas volume fraction of around 0.1. At 3 m/s the transition is shifted to a higher gas fraction of around 0.17. At 4 m/s the influence of the oil drops is qualitatively

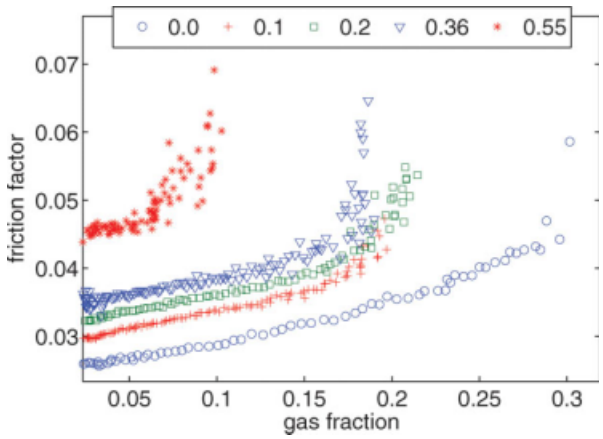

Figure 10. Friction factor for oil–water–gas flows as a function of the gas volume fraction for five different values (0.0, 0.1, 0.2, 0.36, and 0.55) of the oil volume fraction.

Water is the continuous phase. The mixture velocity was 3 m/s. [Color figure can be viewed in the online issue, which is available at www.interscience.wiley.com.]

similar as observed for the case of a mixture velocity of 3 m/s. At 4 m/s the transition starts also at a gas fraction 0.17, but the maximum bubble size is smaller than at a mixture velocity 3 m/s. However, at this velocity even a small change leads to a very strong increase in friction factor. In figure 12 also the probability density function of the bubble size for the experiments at 3 m/s is presented. At a low gas fraction of 0.03 most of the bubbles are small. Increasing the gas fraction increases the bubble size. A strong peak in the bubble size is observed for a gas fraction of 0.12 and 0.18. Despite the fact that at a gas fraction 0.18 the maximum bubble size increases strongly, only a small decrease in the probability of the small bubbles is observed. Most of the bubbles are still small (so the flow is still dispersed). However, the creation of even a small number of large bubbles has a strong influence on the flow (see friction factor in Figure 10).

Continuous experiments with oil as continuous phase

Oil continuous experiments started with pumping oil through the pipe loop and then injecting water in it. After achieving the desired water volume fraction, the water injection was stopped and gas injection started. Figure 13 shows the friction factor as measured during the oil continuous experiments for four different values of the water volume fraction (0.0, 0.37, 0.51, 0.61) and at a mixture velocity 3.5 m/s. The friction factor behaves in the same way as for the water-continuous experiments. It is steadily increasing with increasing gas volume fraction and at the point of transition to elongated bubble flow it becomes very large. Figure 14 presents the maximum bubble size and average bubble size for the oil continuous experiments. As in the previous experiments, also here the transition from dispersed bubble flow to elongated bubble flow is influenced by the presence of the injected liquid in the form of drops. Only this time there is a visible difference between the transition at a water volume fraction of 0.2 and 0.37. This transition occurs at a gas volume fraction of 0.25 and 0.15, respectively. At a dispersed phase volume fraction of 0.51 a dispersed bubble flow is almost impossible, similarly to the water continuous experiments. An injection of a small amount of gas already causes the transition to elongated bubble flow. With air injection it was not possible to maintain a water dispersion at a volume fraction much higher than 0.5. In the oil continuous experiments the influence of the water drops on the average bubble size is stronger than the influence of the oil drops on the bubble size during the water continuous experiments. Furthermore there is another difference. The volume fraction of the water drops has a stronger influence on the bubble size than the volume fraction of the gas bubbles. For the water-continuous flow that was the opposite.

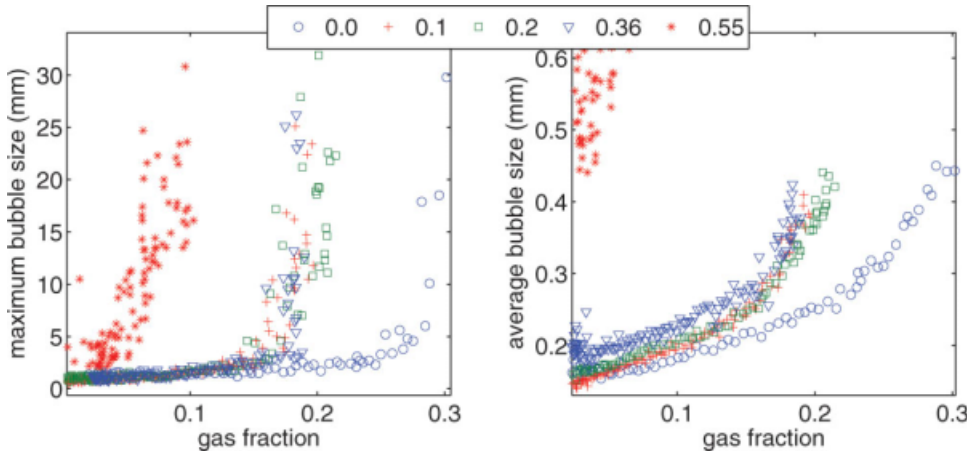

Figure 11. Averaged and maximum bubble size for oil–water–gas flows as a function of the gas volume fraction for five different values (0.0, 0.1, 0.2, 0.36, and 0.55) of the oil volume fraction.

Water is the continuous phase. The mixture velocity was 3 m/s. [Color figure can be viewed in the online issue, which is available at www.interscience.wiley.com.]

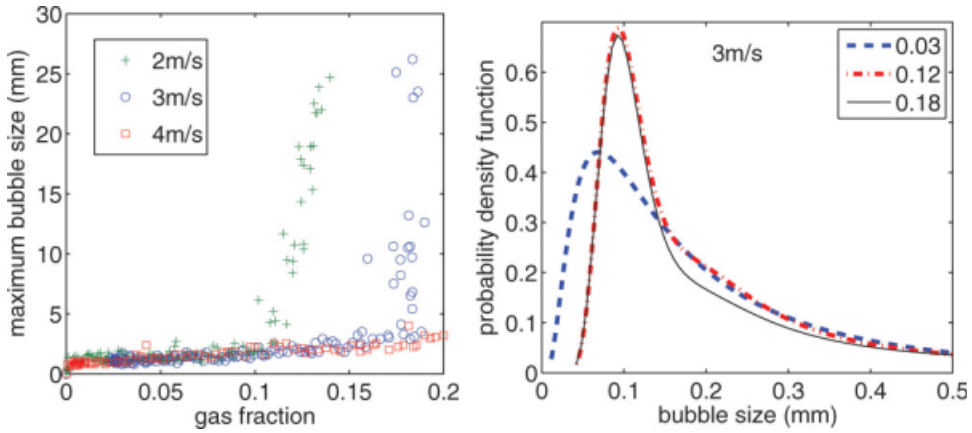

Figure 12. Maximum bubble size for oil–water–gas flows as a function of gas volume fraction for an oil volume fraction of 0.36 and three values (2 m/s, 3 m/s, and 4 m/s) of the mixture velocity.

Water is the continuous phase. In the right figure the probability density function of the gas bubbles for the experiment at the mixture velocity 3 m/s and for three different gas fractions (0.03, 0.12, and 0.18) is presented. [Color figure can be viewed in the online issue, which is available at www.interscience.wiley.com.]

Bubble behavior during phase inversion in a continuous experiment

It is not easy to observe the influence of bubbles on the phase inversion process. During continuous experiments phase inversion only takes place at a high volume fraction of the dispersed phase and as we have shown in the preceding sections dispersed bubble flow is then no longer possible. Furthermore, close to phase inversion it is difficult to control the gas volume fraction, because not only the pressure gradient is high (hence compressibility gets important) but also the continuous adding of dispersed phase liquid during a continuous experiment implies the continuous removal of continuous-phase liquid and gas. A way out to this difficulty is to carry out the experiments in the region where multiple drops are formed. As was shown by Piela et al.[9] when injection of water in an oil continuous flow is stopped at a high water volume fraction (0.54–0.64), production of multiple drops (which entrap parts of the continuous oil phase) increases the effective dispersed phase volume fraction and finally leads to inversion. During such experiments no injection is needed and it is certain that the gas fraction is the same before and after inversion. All experiments were started in the same way as during the continuous oil–water experiments with oil as the continuous phase. The mixture velocity was kept constant at 3.5 m/s. After achieving the desired water volume fraction and gas volume fraction, the injection was stopped and the mixture was circulated through the pipe loop. As with the oil–water experiments the pressure drop was increasing in time up to the inversion point. Figure 15 shows the friction factor, maximum and average bubble size during the phase inversion process. Before inversion the water volume fraction is 0.59. At that fraction dispersed phase flow is not possible. So the average bubble size is large (around 3 mm) and the largest elongated bubbles are of the order of 20–25 mm. Because of the continuous entrapment of oil into the water drops the friction factor increases with time and at time 535 s inversion occurs. During the inversion process the bubbles are quickly broken into small ones, so that after inversion a dispersed bubble flow pattern is observed.

The explanation is likely due to the difference in dispersed phase volume fraction before and after inversion. Before inversion the volume fraction of multiple water drops (with increasing oil droplets inside) is very large ($\geq$0.59) and there is not much space left for the gas bubbles. This causes coalescence of the bubbles and hence creation of large bubbles (slugs). After inversion the volume fraction of oil drops is 0.31 which is much lower (also because oil drops do not easily form multiple drops), which leaves more space and less coalescence for the bubbles in the continuous phase.

During our experiments, we observed a strong influence of the bubbles (slugs) on the phase inversion process in the

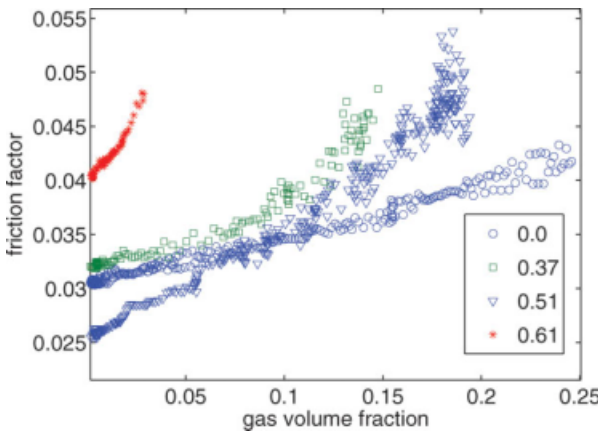

Figure 13. Friction factor for oil–water–gas flows as a function of the gas volume fraction for four different values (0.0, 0.37, 0.51, 0.61) of the water volume fraction.

Oil is the continuous phase. The mixture velocity is 3.5 m/s. [Color figure can be viewed in the online issue, which is available at www.interscience.wiley.com.]

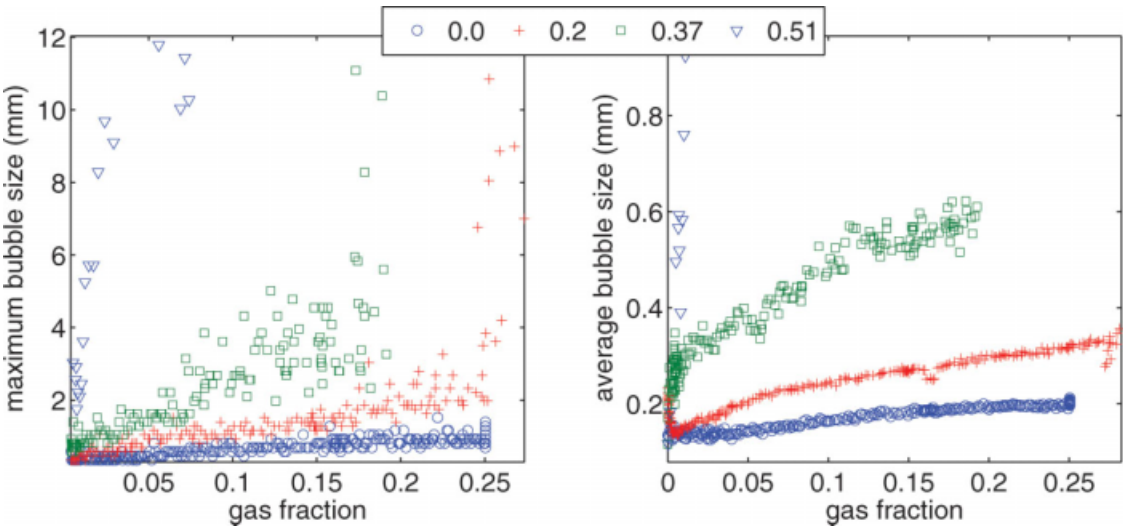

Figure 14. Averaged and maximum bubble size for oil–water–gas flows as a function of the gas volume fraction for four different values (0.0, 0.2, 0.37, 0.51) of the water volume fraction.

Oil is the continuous phase. The mixture velocity is 3.5 m/s. [Color figure can be viewed in the online issue, which is available at www.interscience.wiley.com.]

multiple drop formation region. Figure 16 shows that the presence of gas is slowing down the inversion process. The reason is, that the formation and growth of multiple drops takes place at a lower pace. In the formation and growth process of multiple drops the collision between drops plays an important role and the presence of bubbles decreases the chance on such collisions. This result is important for practical applications. We estimated for a typical case, that the slow down of phase inversion causes the inversion to take place over a pipe length of about 10 km in stead of about 1 km for the case without the presence of gas bubbles. This increased phase inversion length causes a considerable increase of the pressure drop over the production tubing.

Direct experiments

During the direct experiments oil, water and nitrogen gas were simultaneously injected into the pipe at a certain (constant) mixture composition. Inside the pipe both liquids and the gas mix and flow as a three-phase dispersed mixture. As already shown earlier in Figure 7 for a two-phase oil–water flow the friction factor is nearly equal to the friction factor of the single phase flow at all dispersed phase fractions except in the region with an oil volume fraction of 0.5–0.6 where phase inversion occurs. In the phase inversion region the friction factor increases significantly. Figure 17 shows the friction factor and maximum bubble size for two-phase oil–water flows as well as for three-phase flows with a gas

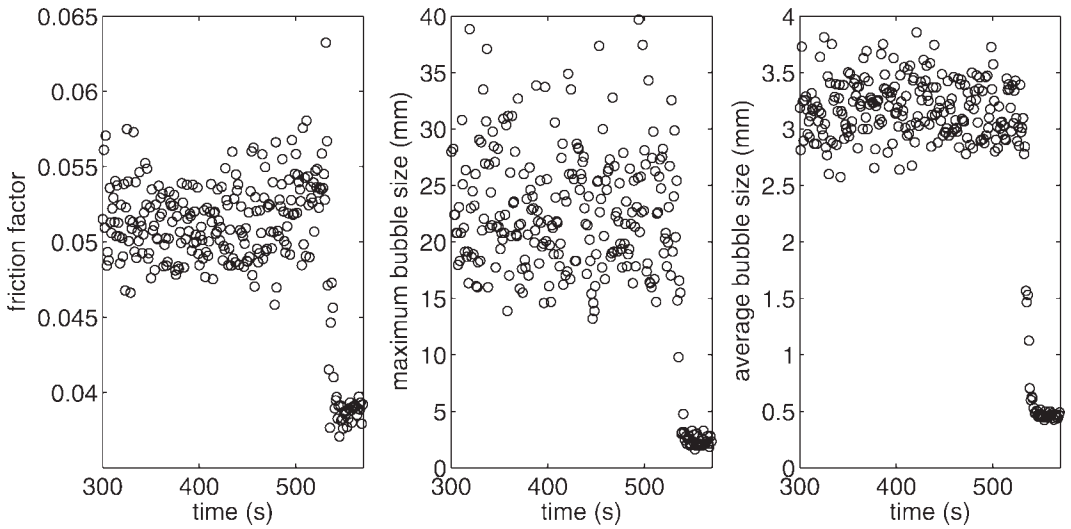

Figure 15. Friction factor, maximum and average bubble size for an oil–water–gas flow during phase inversion.

The water volume fraction is 0.59 and the gas fraction 0.07. Oil is the continuous phase before inversion; water after inversion. The mixture velocity is 3.5 m/s.

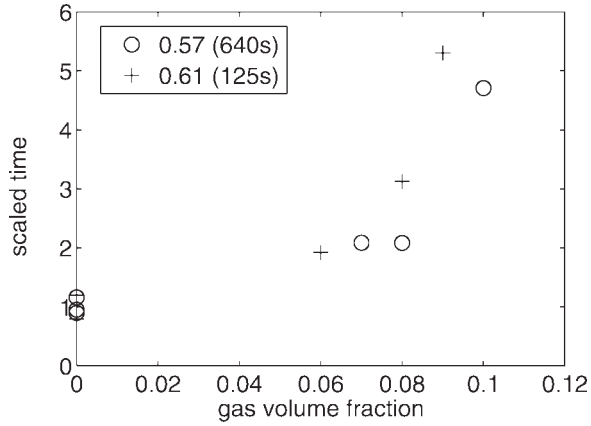

Figure 16. Dimensionless time to inversion for an oil–water–gas flow (made dimensionless by the time to inversion for an oil–water flow) after stopping water and gas injection as a function of the gas volume fraction at a water volume fraction of 0.57 and 0.61.

The time to inversion for an oil–water experiment is 125 s at a water volume fraction of 0.61, and 640 s at a water volume fraction of 0.57.

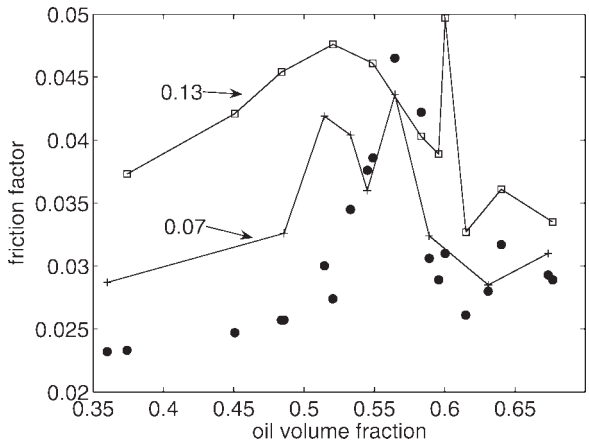

Figure 18. Friction factor for oil–water and oil–water–gas experiments at a mixture velocity 3 m/s and gas volume fractions of 0.07 and 013.

The points represent the oil–water flows and the lines the oil–water gas flows.

volume fraction of 0.03. The mixture velocity was 2 m/s. As can be seen a small amount of gas does not influence the oil–water flow results. Phase inversion still occurs at the same oil volume fraction and the peak in the friction factor and bubbles size remains more or less the same. So the presence of gas is not influencing the inversion process, but this process has a considerable effect on the bubbles as we have discussed before.

Figure 18 shows similar results for the friction factor for a mixture velocity 3 m/s. Although the results for this case are somewhat inaccurate, it seems that phase inversion is still taking place at the same oil volume fraction, but the presence of bubbles increases the friction factor.

Figure 19 shows the variations in time in the friction factor and bubble size during a single direct experiment at oil volume fractions of 0.53 and 0.61. At an oil volume fraction of 0.53 we are in the phase inversion region, at 0.61 we are outside it. At 0.53 strong variations in the friction factor and the maximum bubble size are observed. At phase inversion water and oil continuous regions are continuously created (for more details see our earlier publications), which causes this effect on the friction factor and bubble size. At the higher oil volume fraction of 0.61 oil is the continuous phase with water drops in it. The friction factor is stable and smaller than the friction factor at phase inversion. Also the bubble size is much smaller than in the inversion region.

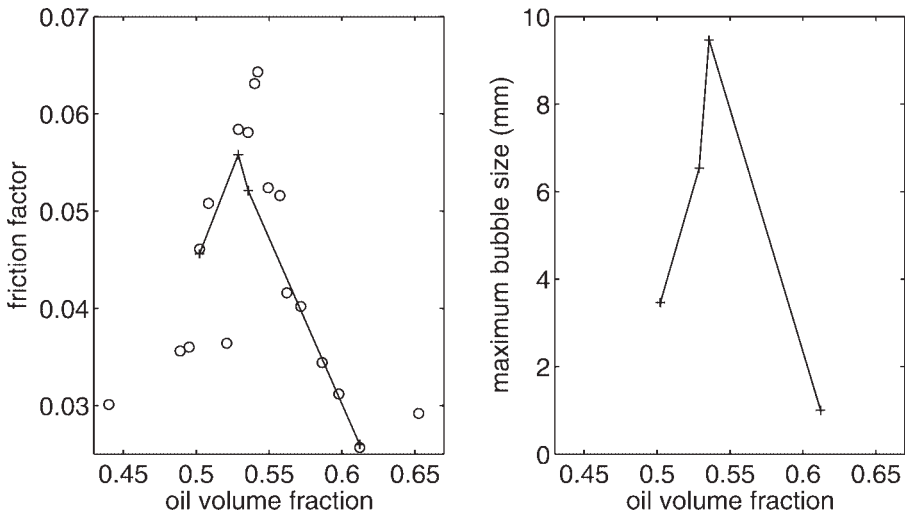

Figure 17. Friction and maximum bubble size factor for oil–water and oil–water–gas experiments at a mixture velocity 2 m/s and gas volume fraction of 0.03.

The open symbols represent the oil–water flows; the line-connected crosses the oil–water–gas flows.

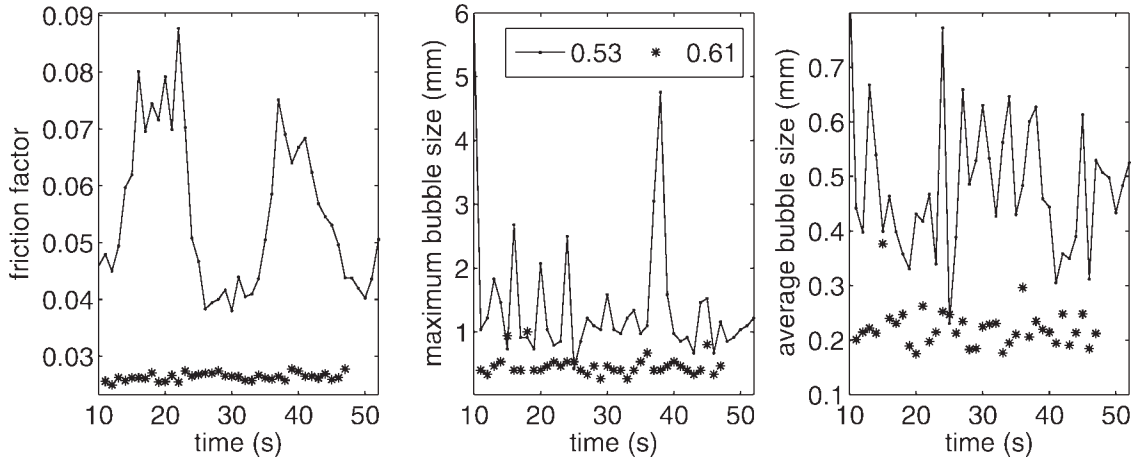

Figure 19. Time variations of the friction factor, maximum bubble size and average bubble size for oil–water–gas experiments at a mixture velocity 2 m/s, a gas volume fraction of 0.03 and at oil volume fractions of 0.53 and 0.61.

Conclusions

In this section a number of points are discussed, that are in our opinion important outcomes of our study.

Let us first discuss the influence of drops on a dispersed bubble flow. We found that the presence of drops causes the transition from dispersed bubble flow to elongated bubble flow at a lower gas volume fraction. This can be explained by the fact, that the drops cause an increase in the effective volume fraction of bubbles in the continuous liquid phase. (Gas bubbles are always present in the continuous liquid phase.) This leads to an increase in bubble coalescence and hence a transition to elongated bubble flows at a lower gas fraction. When the volume fraction of drops is larger than about 0.5, dispersed bubble flow is even not possible anymore. There is a difference, however, between the situations that oil is the continuous phase and that water is the continuous one. In an oil-continuous phase the effect of water drops on the quickening of the transition is stronger than the effect of oil drops when water is the continuous phase. We cannot explain this difference. The calculated bubble size (using the Hinze model[12]) is nearly the same for both types of experiment: 1.3 mm when water is the continuous phase and 1.2 mm when oil is the continuous phase (in agreement with the experimental observations of 0.15 mm and 0.14, respectively.)

A next point is the influence of the phase inversion process on the gas bubbles during a continuous experiment. It is important to point out, that during such experiments the dispersed drop volume fraction at phase inversion is high (much higher than 0.5). So just before inversion a dispersed bubble flow is not possible. Large bubbles are present and the flow pattern is elongated bubble flow. During the inversion process the bubbles break quickly and as the dispersed drop concentration is then much lower than before inversion a dispersed bubble flow is generated. We found that the bubbles do not have a significant effect on the critical volume fraction and pressure gradient at phase inversion, but phase inversion has a strong influence on the bubbles.

Acknowledgments

The authors are grateful to Shell Exploration and Production and the Foundation for Fundamental Research on Matter (FOM) in The Netherlands for the financial support to this project.

Literature Cited

1. Acikgöz M, Franca F, Lahey RT. An experimental study of three-phase flow regimes. *Int J Multiphase Flow*. 1992;18:327–336.
2. Hewitt GF, Pan L, Khor AH. Three-Phase Gas–Liquid–Liquid Flow: Flow Pattern, Hold-up and Pressure Drop. *ISMF* 1997;97:7–10.
3. Wu H, Zhou F, Wu Y. Intelligent identification system of flow regime of oil–gas–water multiphase flow. *Int J Multiphase Flow*. 2001;27:459–475.
4. Spedding PL, Donnelly GF, Cole JS. Three phase oil–water–gas horizontal co-current flow. I. Experimental and regime map. *Chem Eng Res Des*. 2005;83:401–411.
5. Oddie G, Shi H, Durlofsky LJ, Aziz K, Pfeffer B, Holmes JA. Experimental study of two and three phase flows in large diameter inclined pipes. *Int J Multiphase Flow*. 2003;29:527–558.
6. Nädler M, Mewes D. The effect of gas injection on the flow of immiscible liquids in horizontal pipes. *Chem Eng Technol*. 1995;18:156–165.
7. Lahey RT Jr, Acikgöz M, Franca F. Global volumetric phase fractions in horizontal three-phase flows. *AIChE J*. 1992;38:1049–1058.
8. Hewitt GF. Three-phase gas–liquid–liquid flows in the steady and transient states. *Nucl Eng Des*. 2005;235:1303–1316.
9. Piela K, Delfos R, Ooms G, Westerweel J, Oliemans RVA, Mudde RF. Experimental investigation of phase inversion in an oil–water flow through a horizontal pipe loop. *Int J Multiphase Flow*. 2006;32:1087–1099.
10. Piela K, Delfos R, Ooms G, Westerweel J, Oliemans RVA. On the phase inversion process in an oil–water pipe flow. *Int J Multiphase Flow*. 2008;34:665–677.
11. Brauner N. The prediction of dispersed flows boundaries in liquid–liquid and gas–liquid systems. *Int J Multiphase Flow*. 2001;27:885–910.
12. Hinze JO. Fundamentals of the hydrodynamic mechanism of splitting in dispersion processes. *AIChE J*. 1955;1:289–295.
13. Cartellier A. Optical probes for local void fraction measurements: Characterization of performance. *Rev Sci Instrum*. 1990;61:874.
14. Delfos R, Wisse CJ, Oliemans RVA. Measurement of air-entrainment from a stationary Taylor bubble in a vertical tube. *Int J Multiphase Flow*. 2001;27:1769–1787.

15. Cartellier A. Simultaneous void fraction measurement, bubble velocity, and size estimate using a single optical probe in gas–liquid two-phase flows. *Rev Sci Instrum.* 1992;63:5442.
16. Hamad F. An optical probe for measurements in liquid–liquid two-phase flow. *Meas Sci Technol.* 1997;8:1122–1132.
17. Fordham EJ, Holmes A, Ramos RT, Simonian S, Huang SM, Lenn CP. Multi-phase-fluid discrimination with local fibre-optical probes. I. Liquid/liquid flows. *Meas Sci Technol.* 1999;10:1329–1337.
18. Fordham EJ, Simonian S, Ramos RT, Holmes A, Huang SM, Lenn CP. Multi-phase-fluid discrimination with local fibre-optical probes. II. Gas/liquid flows. *Meas Sci Technol.* 1999;10:1338–1346.
19. Fordham EJ, Ramos RT, Holmes A, Simonian S, Huang SM, Lenn CP. Multi-phase-fluid discrimination with local fibre-optical probes. III. Three-phase flows. *Meas Sci Technol.* 1999;10:1347–1352.
20. Descamps MN, Oliemans RVA, Ooms G, Mudde RF. Experimental investigation of three-phase flow in a vertical pipe: Local characteristics of the gas phase for gas-lift conditions. *Int J Multiphase Flow*. 2007;33:1205–1221.
21. Ioannou K, Nydal OJ, Angeli P. Phase inversion in dispersed liquid–liquid flows. *Exp Therm Fluid Sci*. 2005;29:331–339.
22. Pal R. Pipeline flow of unstable and surfactant-stabilized emulsions. *AIChE J*. 1993;39:1754–1764.
23. Hewitt GE, Delhaye JM, Zuber N. *Multiphase Science and Technology*. Vol 2. New York: Hemisphere Publishing Corporation 1986.
24. Andreussi P, Paglianti A, Silva FS. Dispersed bubble flow in horizontal pipes. *Chem Eng Sci*. 1999;54:1101–1107.
25. Descamps M, Oliemans RVA, Ooms G, Mudde RF, Kusters R. Influence of gas injection on phase inversion in an oil–water flow through a vertical tube. *Int J Multiphase Flow*. 2006;32:311–322.

Manuscript received Mar. 20, 2008, and revision received Sept. 18, 2008.